Shock Waves (2010) 20:521–529
DOI 10.1007/s00193-010-0288-5

ORIGINAL ARTICLE

Modelling of detonation cellular structure in aluminium suspensions

A. Briand · B. Veyssiere · B. A. Khasainov

Received: 18 November 2009 / Revised: 20 September 2010 / Accepted: 19 October 2010 / Published online: 10 November 2010

Abstract Heterogeneous detonations involving aluminium suspensions have been studied for many years for industrial safety policies, and for military and propulsion applications. Owing to their weak detonability and to the lack of available experimental results on the detonation cellular structure, numerical simulations provide a convenient way to improve the knowledge of such detonations. One major difficulty arising in numerical study of heterogeneous detonations involving suspensions of aluminium particles in oxidizing atmospheres is the modelling of aluminium combustion. Our previous two-step model provided results on the effect on the detonation cellular structure of particle diameter and characteristic chemical lengths. In this study, a hybrid model is incorporated in the numerical code EFAE, combining both kinetic and diffusion regimes in parallel. This more realistic model provides good agreement with the previous two-step model and confirms the correlations found between the detonation cell width, and particle diameter and characteristic lengths. Moreover, the linear dependence found between the detonation cell width and the induction length remains valid with the hybrid model.

Keywords Detonation · Cellular structure · Two-phase mixtures · Aluminium suspensions · Aluminium combustion

Communicated by L. Bauwens.

This paper is based on work that was presented at the 22nd International Colloquium on the Dynamics of Explosions and Reactive Systems, Minsk, Belarus, July 27–31, 2009.

A. Briand · B. Veyssiere (✉) · B. A. Khasainov
Laboratoire de Combustion et de Détonique, UPR 9028 CNRS,
1 avenue Clément Ader, BP 40109,
86961 Futuroscope-Chasseneuil, France
e-mail: veyssiere@lcd.ensma.fr

1 Introduction

Heterogeneous detonations involving aluminium suspensions have been studied for many years due to their importance for industrial safety policies, military applications and propulsion applications. Like in gaseous detonations, the existence of a cellular structure was experimentally established for mixtures containing aluminium suspensions in oxidizing atmospheres [1,2]. However, the characteristic cell size is noticeably larger due to the slower heat release process provided by heterogeneous burning of solid particles.

Numerical modelling of two-phase detonations has been developed for several years to simulate the cellular structure [3–8]. In a previous work [4], based on the two-step model proposed by Khasainov and Veyssiere [9], the authors calculated detonation cell sizes for both aluminium–air and aluminium–oxygen mixtures. They adjusted kinetic parameters to ensure agreement with available experimental data. It appears from the calculations [4] that, in contrast with gaseous mixtures, for aluminium–gas mixtures, ignition does not occur first in high-pressure zones around the triple points areas. In these zones, particle concentration is the highest due to convection of the solid particles by transverse waves, and, as a result, the local particle temperature is the lowest. Because ignition is controlled by heat exchange between gas and particles, it first occurs outside triple points areas, in regions where low concentration of particles results in high temperature; hence, fast ignition.

Using the model [4], Briand et al. [3] numerically investigated the influence of the characteristic particle parameters on cellular structure in aluminium suspensions. The detonation cell size was found to be proportional to the particle diameter to the power 1.4 for both aluminium–air and aluminium–oxygen mixtures, which is comparable with the results obtained by others [6,7,10]. Moreover, as in gaseous

detonations [11], a linear relationship was found between the detonation cell size and the induction length [3]. In the present paper, we improve our reaction model by incorporating a hybrid model of aluminium combustion based on the model described by Frank-Kamenetzkii [12] and similar to that used for detonation applications by Zhang et al. [8]. The results obtained by both the two-step model and the hybrid model are compared.

2 Numerical modelling

The model is based on the theory of multiphase flows [13]: both gaseous and solid phases are assumed to be continuous media with inter-phase transfer of mass, momentum and energy. Particle volume fraction and particle–particle interactions are ignored. Temperature gradients inside the particles are supposed to be negligible. Balance equations for the heterogeneous medium are as follows:

Gaseous phase

$$\begin{aligned}
&\frac{\partial \rho}{\partial t} + \nabla.(\rho\vec{u}) = J \\
&\frac{\partial \rho\vec{u}}{\partial t} + \nabla.((\rho\vec{u}) \otimes \vec{u}) = -\nabla p + J\vec{v}_\mathrm{p} - \vec{f} \\
&\frac{\partial E}{\partial t} + \nabla.(\vec{u}(E+p)) = J(E_\mathrm{p}/\sigma + Q) - \vec{f}.\vec{v}_\mathrm{p} - q
\end{aligned} \tag{1}$$

Solid phase

$$\begin{aligned}
&\frac{\partial \sigma}{\partial t} + \nabla.\left(\sigma\vec{v}_\mathrm{p}\right) = -J \\
&\frac{\partial \sigma\vec{v}_\mathrm{p}}{\partial t} + \nabla.\left((\sigma\vec{v}_\mathrm{p}) \otimes \vec{v}_\mathrm{p}\right) = \vec{f} - J\vec{v}_\mathrm{p} \\
&\frac{\partial E_\mathrm{p}}{\partial t} + \nabla.\left(\vec{v}_\mathrm{p}E_\mathrm{p}\right) = q - JE_p/\sigma + \vec{f}.\vec{v}_\mathrm{p}
\end{aligned} \tag{2}$$

Particle number balance equation

$$\frac{\partial n_\mathrm{p}}{\partial t} + \nabla.\left(n_\mathrm{p}\vec{v}_\mathrm{p}\right) = 0 \tag{3}$$

with

ρ : the gas density
u : the gas velocity vector
J : the mass exchange rate between gas and particles
p : the pressure
v_p : the particle velocity vector
f : the momentum exchange rate between gas and particles
E : the total energy of gas, $E = \rho(e + \frac{1}{2}\vec{u}\cdot\vec{u})$
E_p : the total energy of particles, $E_\mathrm{p} = \sigma(e_\mathrm{p} + \frac{1}{2}\vec{v}_\mathrm{p}.\vec{v}_\mathrm{p})$
e_p : the internal energy of particles
Q : the heat of reaction
q : the energy exchange rate between gas and particles
σ : the apparent density of particles
n_p : the particle number density

Detonation products balance equation

$$\frac{\partial \rho_\mathrm{rp}}{\partial t} + \nabla.\left(\rho_\mathrm{rp}\vec{u}\right) = (1+\chi)J \tag{4}$$

with

ρ_rp : the density of detonation products
χ : the stoichiometric coefficient

Interactions between gaseous and solid phases

2.1 Mass exchange

Our previous two-step model for aluminium combustion [9] presented the advantage to easily separate the induction and combustion periods, which allows to study their respective effects on the detonation cellular structure [3]. Similar simplified models were also used in studies, such as [5,6]. However, they require defining a particle ignition temperature which plays an important role, below which the reaction rate is set to zero and above which combustion occurs. Thus, this approach requires identifying an appropriate ignition criterion for aluminium particles. The choice of the ignition temperature was examined in [14]; as a result, here it was set to 1,350 K.

The hybrid model incorporated in our current model is similar to that proposed by Zhang et al. [8] for aluminium–air detonations. It combines both kinetic and diffusion regimes [12] for aluminium combustion. As such, it is more realistic than these previous models, and it does not depend on an ignition criterion. The overall burning rate J controls both ignition and combustion periods, according to the following equation:

$$J = \left(\frac{1}{J_\mathrm{kin}} + \frac{1}{J_\mathrm{diff}}\right)^{-1} \tag{5}$$

in which the burning rates of the kinetic regime J_{kin} and diffusion regime J_{diff} are, respectively, defined as follows:

$$\begin{cases}
J_\mathrm{kin} = \pi d_\mathrm{p}^2 n_\mathrm{p} Z_\mathrm{hyb} \exp\left(-\frac{E_\mathrm{a}}{RT_\mathrm{p}}\right) \\
J_\mathrm{diff} = 3\sigma\left(1 + 0.276\sqrt{Re}\right)/\tau_\mathrm{p}
\end{cases} \tag{6}$$

with

d_p : the particle diameter
Z_hyb : the pre-exponential factor
E_a : the activation energy
R : the universal gas constant
T_p : the particle temperature
Re : the Reynolds number
τ_p : the burning time

In the hybrid model, the temperature in the Arrhenius rate is the particle temperature T_p. Zhang et al. [8] proposed the use of the "film" temperature $T_{film} = (T_p + T_g)/2$ as the temperature in the Arrhenius rate. The difference between these two models becomes significant only for larger particles ($d_p > 50\mu$m) when internal temperature gradients and thermal non-equilibrium with the surrounding gas becomes large. In the present work, we consider only particles of smaller diameter for which the assumption of uniform temperature inside the particles is fully justified.

The definition of the Reynolds number is given by:

$$Re = d_p \left|\vec{u} - \vec{v}_p\right| / \upsilon_g \tag{7}$$

where υ_g is the kinematic viscosity.

The burning time τ_p is defined according to Price [15] as:

$$\tau_p = \frac{K d_{p0}^2}{\phi_{ox}^{0.9}} \tag{8}$$

with

K : the particle burning time constant
ϕ_{ox} : the molar fraction of oxidant in gaseous phase

2.2 Momentum exchange

Gas and particle velocities are equilibrated by the drag force f given by (9), in which the particle drag coefficient C_d is given, according to Nigmatulin [13], by (10):

$$\vec{f} = \frac{3}{4}\frac{\rho}{\rho_p}\frac{\sigma_p}{d_p} C_d \left(\vec{u} - \vec{v}_p\right)\left|\vec{u} - \vec{v}_p\right| \tag{9}$$

where ρ_p is the particle material density.

$$C_d = \frac{24}{Re} + \frac{4.4}{\sqrt{Re}} + 0.42 \tag{10}$$

2.3 Heat exchange

The heat exchange q between gas and particle includes both convective and radiative contributions. It is given by (11):

$$q = \frac{6\sigma}{\rho_p d_p}\left[\frac{Nu\lambda_g\left(T - T_p\right)}{d_p} + \varepsilon\sigma_{Boltz}\left(T^4 - T_p^4\right)\right] \tag{11}$$

Here the Nusselt number Nu is defined, according to Nigmatulin [13], by (12), where the Prandtl number Pr is given by (13):

$$Nu = 2 + 0.6 Pr^{1/3}\sqrt{Re} \tag{12}$$

$$Pr = \frac{\mu_g c_p}{\lambda_g} \tag{13}$$

with

λ_g : the thermal conductivity of the gas
T : the gas temperature
ε : the emissivity of the particle
σ_{Boltz} : the Boltzmann constant
μ_g : the dynamic viscosity of the gas
c_p : the gas heat capacity at constant pressure

The emissivity of the particle suspension has been examined in [16] and it was found in [9] that the contribution of the radiative part to the heat exchange term q can be neglected.

The particle diameter is calculated from (14):

$$d_p/2 = \sqrt[3]{\sigma_p \Big/ \left[\frac{4\pi}{3}\rho_p n_p\right]} \tag{14}$$

Finally, the equations of state for the gas phase are

$$p = \rho R\left(\frac{1 - x_{rp}}{w_g} + \frac{x_{rp}}{w_{rp}}\right) T \tag{15}$$

$$e = \left[c_{v_g}\left(1 - x_{rp}\right) + c_{v_r p} x_{rp}\right] T \tag{16}$$

Here indexes $()_g$ and $()_{rp}$, respectively, refer to the initial (fresh) gas and to the reaction products x_{rp} whose mass fraction in the gaseous phase is defined as

$$x_{rp} = \rho_{rp}/\rho \tag{17}$$

and c_v is the heat capacity at constant volume, while w is the molecular mass.

The detonation is considered as a wave of finite thickness, where the chemical reactions are initiated by the leading shock wave and their progress is controlled by the interphase exchanges of mass, impulse and energy between particles and gases.

3 Numerical method

The system of 2D equations (1–17) is solved in cylindrical $x-r$ coordinates using an Eulerian grid. The home-made numerical code EFAE uses an explicit finite difference scheme based on the flux-corrected transport method from Oran and Boris [17] to ensure monotonicity, and stability is assured by the Courant–Friedrichs–Lewy criterion [18]. The radial grid has a uniform size Δr at any longitudinal coordinate x. Along the propagation direction x, an adaptation technique is implemented: half of the grid with fixed size $\Delta x_{fine} = \Delta r$ is used around the detonation front, where physical lengths and time scales are the smallest [19], providing an accurate discretization of the reaction zone. Downstream, beyond the zone with square meshes, the other half of the grid is made of cells of variable longitudinal length: Δx is monotonously increased from the finely resolved zone toward the closed end of the tube at $x = 0$ ($i = 1$). Thus, at a given number of longitudinal cells N_x, $\Delta x = \Delta x_{fine}$ at

$i = N_x/2, N_x/2+1, \ldots, N_x$ and $\Delta x_i = (1+\varepsilon)\Delta x_{i+1}$ at $i = N_x/2-1, N_x/2-2, \ldots, 1$ where ε is a small parameter whose value slowly grows with every adaptation. The mesh size Δx_i near the closed wall (i=1, 2, …) is not allowed to exceed O($D{\cdot}t$/100) where $D{\cdot}t$ is the run distance of the leading front. The grid adaptation and corresponding re-mapping of flow parameters is done every time the shock front arrives at the right boundary $i = N_x$ of the grid. The transverse mesh size Δr is always equal to the smallest longitudinal size Δx_{fine}. With this method, the aforementioned system of equations of the reactive flow can be accurately solved taking into consideration the multiscale character of the problem. Indeed, it allows for long propagation distances while providing a fine resolution in the reaction zone, with reasonable calculation times.

For simulating the detonation cellular structure, one-dimensional planar calculations are first performed up to a quasi-stationary and autonomous detonation regime is reached. Then, this 1D solution is used as an initial condition of a two-dimensional calculation in a cylindrical configuration with a tube of small diameter (about $10\Delta x_{\text{fine}}$), and the calculation is advanced until numerical perturbations appear and give rise to the formation of triple points. This process is repeated by increasing the tube diameter until calculations display the quasi-steady detonation cellular structure in the tube. Then, this solution is replicated in the radial direction providing an initial condition for another 2D problem, but in a larger channel. The tube dimension in the final simulation is chosen such that the detonation cell width becomes independent of the tube size. This method yields the detonation structure after a stationary and autonomous regime has been reached, in reasonable calculation time. The final detonation cellular structure does not depend on the process whereby the tube diameter was increased before reaching the final solution, affecting neither velocity or structure.

In the following simulations, the particle radius is typically of the order of a few micrometers. The numerical resolution (i.e. Δx_{fine}) depends on particle size and is chosen to provide at least a few tens of numerical cells in the induction zone (typically Δx_{fine} is of the order of the millimeter [3]).

Simulation of the cellular structure of aluminium particles— oxygen detonation has been already attempted in the past [5], but the tube diameter (12 cm) and length (60 cm) chosen for that study were clearly too small to allow obtaining a steady propagation regime and a cell size independent of the tube dimension. Conclusions reached in [6,7] may be due to insufficient resolution, in the absence of detailed information. The few available experimental results in aluminium particle–air mixtures [1] show a detonation propagating in the spinning mode, due to the narrow size of the tube. The spinning detonation regime in aluminium suspensions would require a specific investigation; it is not examined here.

4 Reference mixtures

Two reference mixtures are considered, based on the experimental data of Zhang et al. [1] for aluminium–air mixtures and those of Ingignoli et al. [2] for aluminium–oxygen mixtures. Energetic parameters of those two mixtures were determined using the thermodynamic calculations with the TDS code [20]. Namely, for the aluminium–air mixture at concentration $\sigma = 500\,\text{g/m}^3$ the ideal CJ detonation velocity is $D_{\text{CJ}} = 1{,}742\,\text{m/s}$, the molecular mass of detonation products $w_{\text{CJ}} = 0.03849\,\text{kg/mol}$ and their heat capacity $(c_{\text{v}})_{\text{CJ}} = 1{,}751\,\text{J/kg/K}$. Similarly, for the aluminium–oxygen mixture at concentration $\sigma = 1{,}500\ \text{g/m}^3$, the detonation velocity is $D_{\text{CJ}} = 1{,}592\,\text{m/s}$, $w_{\text{CJ}} = 0.04979\,\text{kg/mol}$ and $(c_{\text{v}})_{\text{CJ}} = 1{,}756\,\text{J/kg/K}$.

As for the previous two-step model, three parameters have to be set to describe the chemistry of aluminium combustion. Two of them are taken from the literature: the burning time constant K is set to the same value as in our former two-step model: $K = 1.6 \times 10^6\,\text{s/m}^2$, as proposed by Ingignoli [21] for flake-type particles. In addition, the activation energy of the kinetic regime in the mass exchange source term is also set to the same value as before, in the case of reaction between aluminium and oxygen, according to the measurements of Merzhanov et al. of aluminium wires combustion [22]: $E_{\text{a}} = 17{,}000\,\text{cal/mol}$. Thus, as for the two-step model, the only free parameter requiring fitting is the pre-exponential factor Z_{hyb} in the kinetics. For both aluminium–air and aluminium–oxygen mixtures, Z_{hyb} was varied in a wide range to compare the calculated detonation cell widths with available experimental data and to those simulated by Veyssiere et al. [4].

The aluminium–air reference mixture corresponds to the experiments of Zhang et al. [1] with flake particles (with estimated equivalent diameter $d_{\text{p}} = 13.5\,\mu\text{m}$) at standard pressure and temperature. For a rich mixture (equivalence ratio 1.61) and particle concentration $\sigma = 500\ \text{g/m}^3$, the measured detonation cell width is $\lambda \approx 40\,\text{cm}$ [1] and for the pre-exponential factor in the hybrid model the best-fit value is $Z_{\text{hyb}} = 7.5 \times 10^4\ \text{kg/m}^2\text{/s}$.

For stoichiometric aluminium–oxygen mixture ($\sigma = 1{,}500\ \text{g/m}^3$) at standard pressure and temperature, Ingignoli et al. [2] recorded a detonation cell with a characteristic width $\lambda \approx$ 5–10 cm for flake particles (with estimated equivalent diameter $d_{\text{p}} = 8.6\,\mu\text{m}$). Here, the best-fitting value of the pre-exponential factor for the hybrid model is $Z_{\text{hyb}} = 3 \times 10^6\,\text{kg/m}^2\text{/s}$. The larger value of Z_{hyb} for the oxygen–aluminium mixture may be due to the smaller size and larger concentration of particles and to the higher oxygen concentration. There remains significant uncertainty about detonation cell size for oxygen–aluminium mixtures, because experimental data are very limited.

Initiation is achieved by a point explosion source with an energy of the order of 0.1 MJ/m^2 at $t = 0$ at the left closed end of the tube. The initiation energy was chosen to be nearly twice the critical initiation energy which depends on mixture reactivity and drops as the particle size is reduced.

5 Comparison of 1D simulations using two-step model and hybrid model

Figures 1 and 2, respectively, show for aluminium–air and aluminium–oxygen mixtures the evolution of detonation velocity in the tube, for the hybrid model. For both mixtures, the run time to a quasi-steady detonation regime is at least 2 ms, which corresponds to a run distance of approximately 4 m (this already indicates significantly lower reactivity of aluminum suspensions in air or oxygen, in comparison with typical gaseous explosive mixtures). After this rather long transient period, the mean detonation velocity approaches $D = 1{,}740$ m/s for the aluminium–air mixture (Fig. 1), which is only 0.1% below the ideal value $D_{CJ} = 1{,}742$ m/s (see previous section). Fluctuations of velocity of the self-supported detonation caused by the Arrhenius character of chemical reactions do not exceed 1.5%. For the aluminium–oxygen mixture (Fig. 2), the hybrid model also gives good agreement between the mean detonation velocity $D = 1{,}594$ m/s and the ideal one $D_{CJ} = 1{,}592$ m/s.

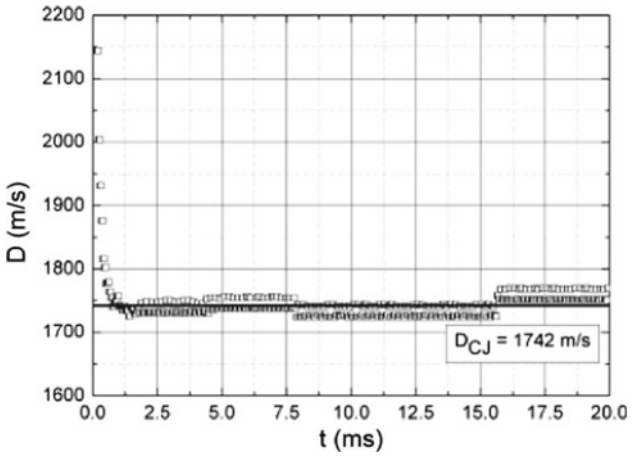

Fig. 1 Evolution of the detonation velocity for the hybrid model in the case of aluminium–air mixture (richness 1.61, equivalent particle diameter 13.5 μm)

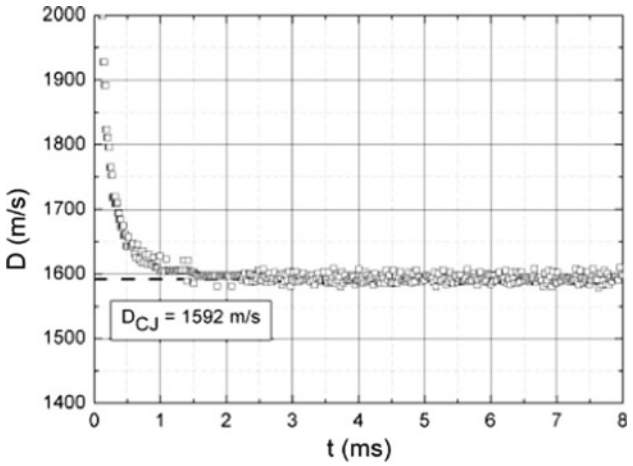

Fig. 2 Evolution of the detonation velocity for the hybrid model in the case of aluminium–oxygen stoichiometric mixture (equivalent particle diameter 8.6 μm)

Figure 3 displays the evolution of the main flow parameters behind the leading front.

The agreement between the results obtained with the two models is very good. The differences observed in particle temperatures immediately after the ignition have no physical meaning. Indeed, they are due to the fact that in the two-step model, the particle temperature continues to increase rapidly according to Arrhenius law even after particle ignition: as this parameter is not used in the subsequent calculations of the diffusion step, particle temperature after ignition is arbitrarily limited to 2,000 K just to indicate conveniently the burning stage of the process. Figure 3 compares for both models the evolution of mass exchange rates for aluminum–air mixtures, with $X = Dt - x$, i.e. a longitudinal coordinate attached to the detonation front. The estimated induction length is about $L_i = 3.5$ cm for the hybrid model and 4.5 cm for the two-step model while the combustion zone length is of the order of $L_c = 40$ cm for both models. The induction length is defined here as the distance between the leading front and the point where the gradient of particle temperature becomes maximum, whereas the combustion length goes from the moment when the relative decrease in the particle radius becomes noticeable (here >0.1%) to the point where this radius becomes smaller than 10% of the initial radius. The particle radius decreases similarly for both models. The

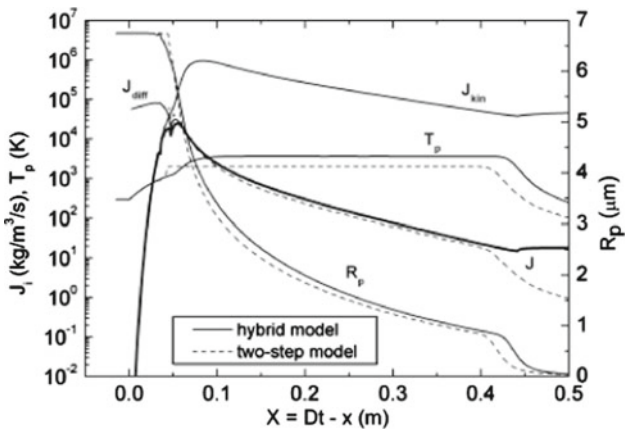

Fig. 3 Combustion regimes and ignition parameters for aluminium–air mixture

burning rates J are also similar up to $X = 0.40$ m. Beyond that value, J corresponding to the two-step model drops faster (due to a numerical criterion used to treat the final stage of the particle burn-out, when its radius approaches zero), but this has no influence on the global energy release since the particle radius at that moment is as small as 10% of its initial value, so that 99.9% of the initial particle mass has already been burnt, and the burning rate is three orders of magnitude smaller than the corresponding maximum value immediately after ignition.

Despite the different definitions of the combustion rates for both models, they lead to very close results. A transition period of approximately 3-cm length is observed for the hybrid model where the mass exchange rate J progressively changes from the kinetic regime J_{kin} (lasting from $X = 0$ to $X = 4.1$ cm) to the diffusive regime J_{diff} (for $X > 7$ cm). Finally, the effective ignition temperature of particles which is derived from calculations for the hybrid model is close to 1,100 K, which is slightly smaller, but consistent with the value chosen here in the calculations with the two-step model (1,350 K), and comparable with the values found in the literature. Profiles of other main flow parameters, such as pressure, particle and gas density, and temperature inside the reaction zone and further downstream are practically identical.

6 Simulation of the detonation cellular structure with the hybrid model

Typical cellular structures, obtained by numerical simulations performed using the hybrid model with the aforementioned set of input parameters, are displayed in Figs. 4 and 5, for a tube diameter large enough to allow for a sufficient number of detonation cells to exist across the tube radius, ensuring that the cell width is independent of the diameter (see above section). In both cases, due to the cylindrical geometry of the flow, an implosion of converging triple points at the axis of symmetry induces strong reflected waves. For the aluminium–air mixture (see Fig. 4), the cellular structure appears to be less regular than with the two-step model: except along the axis, the cellular network is composed of cells of variable dimension, either decreasing or increasing along the axial and the radial coordinates. The average size is chosen as the characteristic cell width, resulting in $\lambda \approx 40 \pm 10$ cm. For aluminium–oxygen mixture (see Fig. 5), cells are nearly regular and the characteristic width is $\lambda \approx 10 \pm 1$ cm. These results are in reasonable agreement with experimental observations. When compared with our previous calculations with the two-step model [4], the present values are slightly larger. In both cases, the ratio λ/L of the cell width to its length vary in a range of [0.43, 0.5], which is smaller than for homogeneous gaseous detonations ($\lambda/L \approx 0.6$). The tracks of triple point trajectories appear to be significantly

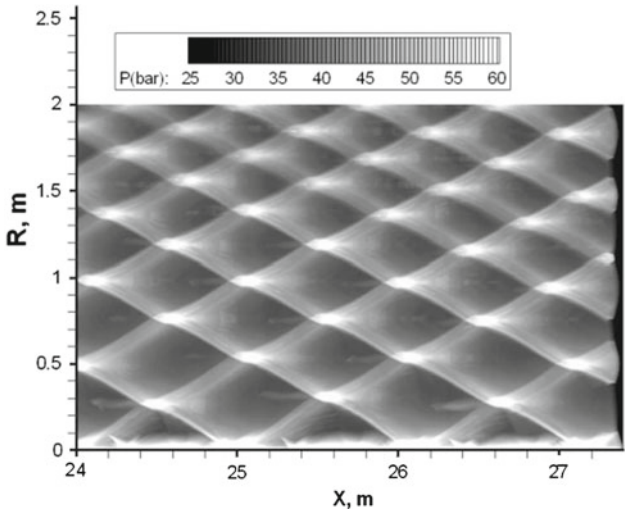

Fig. 4 Detonation cells obtained using the hybrid model for aluminium–air mixture (richness 1.61, equivalent particle diameter 13.5 μm)

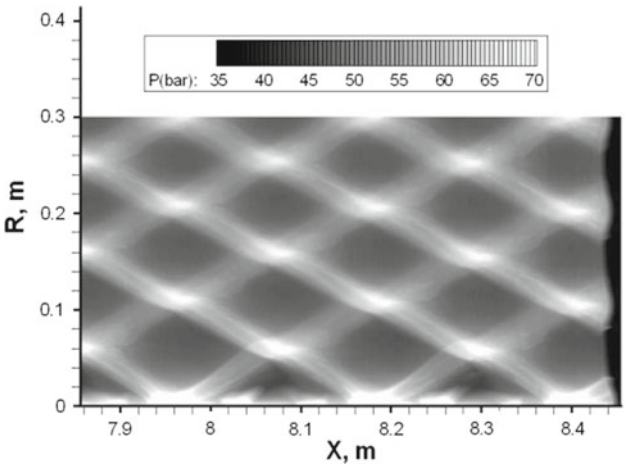

Fig. 5 Detonation cells obtained using the hybrid model for aluminium–oxygen stoichiometric mixture (equivalent particle diameter 8.6 μm)

thicker than in gaseous mixtures, particularly for the oxygen–aluminium mixture. This could be attributed to the relaxation process, but also to a longer reaction time for Al suspensions in comparison with typical gaseous explosives. Indeed, this thickness is about 10 cm in Al/air mixture and about 2.5 cm in Al/O_2 case. The ratio of these thicknesses is close to that of detonation cell sizes showing that aluminium suspensions in oxygen are markedly more reactive than in air.

7 Influence of the particle diameter on the characteristic chemical lengths

Previous results [3] obtained with the two-step model showed that the induction and combustion zone lengths are,

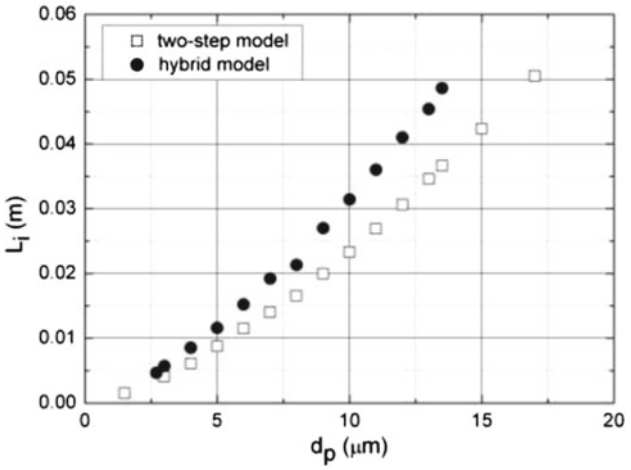

Fig. 6 Induction length as function of particle diameter for both models (aluminium–air mixture)

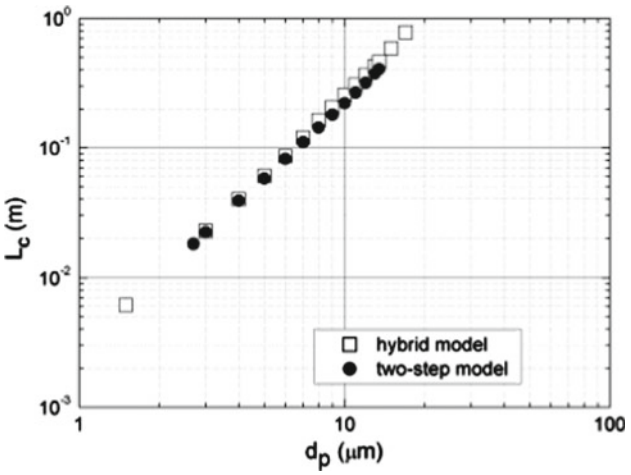

Fig. 7 Combustion zone length as function of particle diameter for both models (aluminium–air mixture)

respectively, proportional to the particle diameter and to the particle diameter to the power 1.8. With the present hybrid model, numerical simulations have been performed for aluminium–air mixtures, varying the particle diameter from 1.5 to 17 μm. For these calculations, the numerical mesh size in the well-resolved zone of the detonation wave ranged from 0.1 to 2.5 mm to ensure that at least ten numerical cells were included in the induction length. Figures 6 and 7 display the influence of the particle diameter, respectively on the induction length and on the combustion zone length for both models, in the 2D case.

The relationship between induction length and particle diameter is found to be $L_i \sim d_{p0}^{n_i}$, with $n_i = 1.42$ for the hybrid model and $n_i = 1.36$ for the two-step-model (Fig. 6). In both cases, the dependence of L_i on d_{p0} can be approximately represented in the range of parameters under consideration as $L_i \sim d_{p0}^{1.4}$. For the two-step model, this type of relationship was to be expected because of the ignition model (see [3]). However, for the hybrid model, the reaction rate is by definition (6) inversely proportional to the instantaneous particle diameter (since n_p is inversely proportional to d_p^3). Even so, the qualitative agreement between the two models is quite good, despite the different definitions. Still, the induction lengths obtained with the two-step model at a chosen value of ignition temperature are higher than those obtained with the hybrid model, the difference between the results being larger for larger particles.

Figure 7 shows quantitative agreement between both models as far as the combustion zone length is concerned. This behavior could be expected, due to the same definition of the diffusive regimes for the two models. The combustion zone length is proportional to the particle diameter to the power 1.8, which is quite close to the definition given by Eq. (8).

8 Correlations for the detonation cell size

Briand et al. [3] have used the two-step model and found that the detonation cell width is proportional to the particle diameter to the power 1.4. Figure 8 compares these results with those obtained with the hybrid model. It appears that the same correlation can be derived here $\lambda \sim d_{p0}^{1.4}$. In the previous section, we have found a similar dependence for $L_i \sim d_{p0}^{1.4}$, hence a linear correlation between λ and L_i. Values of the cell width for both models are close but slightly higher with the hybrid model, in agreement with previously proposed correlations between induction length and combustion zone length. In [6,7], a correlation $\lambda \sim d_{p0}^{1.6}$ was proposed, whereas in [8], a correlation taking initial pressure into consideration is suggested: $\lambda \sim d_{p0}^{n}/p_0^{m}$ with $n > 2$ and $m > 1$. Thus, this dependence of λ on particle diameter remains an open question and necessitates further studies; especially, more detailed and precise experimental data.

These results naturally lead to an attempt to find a correlation between the detonation cell width and the induction length, as proposed by Shchelkin and Troshin [10] for gaseous mixtures or by Briand et al. [3] for aluminium–air and aluminium–oxygen mixtures with the two-step model. Although a proportionality constant k of the order of 7 was obtained in [3] in various conditions, the hybrid model provides a higher value of about 11 for aluminium–air mixtures, as shown in Fig. 9. This difference in k is the consequence of slightly higher values of λ and smaller values of L_i produced by the hybrid model. Thus, taking into consideration the different definitions of the mass exchange rates in the two models, one can generalize the aforementioned correlation between λ and L_i for both mixtures as

$$\lambda \approx 10\, L_i \tag{18}$$

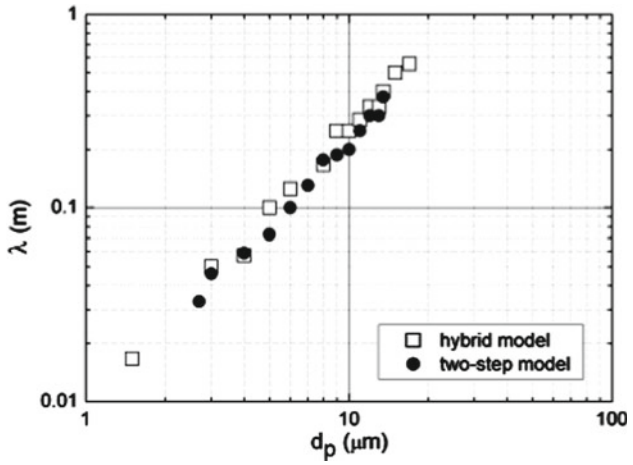

Fig. 8 Detonation cell size as function of particle diameter for both models (aluminium-air mixture)

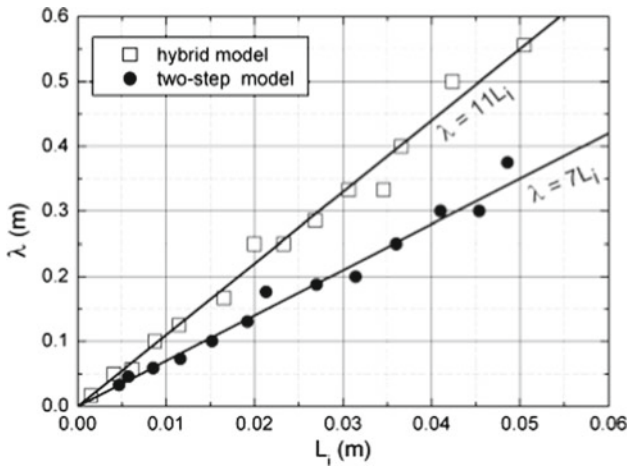

Fig. 9 Detonation cell size as function of induction length for both models (aluminium–air mixture)

9 Conclusions

Good agreement was observed between detonation cellular structures in aluminum/air and aluminum/oxygen mixtures calculated using the hybrid model, and those previously obtained with the two-step model. This confirms the reliability of the two-step model as well as previous results based on the two-step model [3,4]. However, the hybrid model appears to be more convenient for aluminium combustion modelling, since it leads to particle ignition being automatically controlled by the transition between the kinetic-limited regime and the diffusion-limited burning regime. The hybrid model does not depend on a somewhat arbitrary choice of a particle ignition temperature behind a shock wave and corroborates the conclusions of Zhang et al. [7]. The hybrid model confirms that the detonation cell width is proportional to the particle diameter to the power 1.4 while the induction and combustion zone lengths are, respectively, proportional to the particle diameter to the power 1.4 and to the power 1.8. The linear dependence of the detonation cell width on the induction length is also confirmed.

References

1. Zhang, F., Grönig, H., Van de Ven, A.: DDT and detonation waves in dust–air mixtures. Shock Waves **11**, 53–71 (2001)
2. Ingignoli, W., Veyssiere, B., Khasainov, B.A.: Shock initiation of detonations in aluminium–oxygen mixtures. In: Pulsed and Continuous Detonations, pp. 218–224. Torus Press, Moscow, ISBN 5-94588-040-X (2006)
3. Briand, A., Veyssiere, B., Khasainov, B.A.: Detonability of aluminium suspensions. In: Proceedings of the 7th ISHPMIE, vol. 2, pp. 213–222. St. Petersburg, Russia (2008)
4. Veyssiere, B., Khasainov, B.A., Briand, A.: Investigation of detonation initiation in aluminium suspensions. Shock Waves **18**(4), 307–315 (2008)
5. Benkiewicz, K., Hayashi, A.K.: Two-dimensional numerical simulations of multi-headed detonations in oxygen–aluminium mixtures using adaptative mesh refinement. Shock Waves **12**(5), 385–402 (2003)
6. Fedorov, A.V., Khmel, T.A.: Numerical simulation of formation of cellular heterogeneous detonation of aluminium particles in oxygen. Comb. Expl. Shock Waves **41**(4), 435–448 (2005)
7. Khmel, T.A., Fedorov, A.V.: Dependence of the heterogeneous detonation cell size on the flow scales. In: Roy, G., Frolov, S.M. (eds.) Pulse and Continuous Detonation Propulsion, pp. 107–122. Torus Press, Moscow (2006)
8. Zhang, F., Gerrard, K.B., Ripley, R.C., Tanguay, V.: Unconfined aluminium particles–air detonation. In: Proceedings of the 26th ISSW, pp. 15–20. Goettingen, Germany (2007)
9. Khasainov, B.A., Veyssiere, B.: Analysis of the steady double-front detonation structure for a detonable gas laden with aluminium particles. Arch. Combust. **7**(3–4), 333–352 (1987)
10. Zhang, F., Murray, S.B., Gerrard, K.B.: Aluminium particles–air detonation at elevated pressure. Shock Waves **15**, 313–324 (2006)
11. Shchelkin, K.I., Troshin, Ya.K.: Gas-Dynamics of Combustion [in Russian]. Izd. Akad. Nauk. SSSR, Moscow (1963)
12. Frank-Kamenetzkii, D.A.: Diffusion and Heat Transfer in Chemical Kinetics. Plenum Press, New York (1969)
13. Nigmatulin, R.I.: Prikl. Matemat. Mekh. **34**, 1097–1112 (1970)
14. Veyssiere, B., Khasainov, B.A.: A model for steady, plane, double-front detonations (DFD) in gaseous explosive mixtures with aluminium particles in suspension. Combust. Flame **85**, 241–253 (1991)
15. Price, E.W.: Combustion of metalized propellants, fundamentals of solid propellant combustion. In: Kuo, K.K., Summerfield, M.M. (eds.) Progress in Astronautics and Aeronautics, vol. 90, pp. 479–513. AIAA, New York (1984)
16. Veyssiere, B., Kato, Y., Brochet, C., Bouriannes, R., Manson, N.: Pyrometric studies of Al combustion in the wake of two-phase detonations. Arch. Combust. **3**(3), 151–160 (1983)
17. Oran, E.S., Boris, J.P.: Numerical Simulation of Reactive Flow, 2nd edn. Cambridge University Press, Cambridge (2001)
18. Hirsch, C.: Numerical Computation of Internal and External Flows. Vol. 1: Fundamentals of Numerical Discretization. Wiley, New York (1988)
19. Veyssiere, B., Bozier, O., Khasainov, B.A.: Effect of a suspension of magnesium particles on the detonation characteristics of methane-oxygene-nitrogen mixtures at elevated initial pressure. Shock Waves **12**, 27–233 (2002)

20. Victorov, S.B., Gubin, S.A.: A double-front structure of detonation wave as the result of phase transition. Shock Waves **15**(2), 113–128 (2006)
21. Ingignoli, W.: Etude de la formation et de la propagation des detonations dans des suspensions de particules d'aluminium en atmosphere oxydante ou reactive. These de Docteur-Ingenieur, ENSMA, University of Poitiers, France (1999)
22. Merzhanov, A.G., Grigor'jev, Yu.M., Gal'Chenko, Yu.A.: Aluminium ignition. Combust. Flame **29**, 1–14 (1977)